



# Quantum propagator approach to heavy-ion fusion

J-D. Bao, D. Boilley

## ► To cite this version:

J-D. Bao, D. Boilley. Quantum propagator approach to heavy-ion fusion. Nuclear Physics A, 2002, 707, pp.47-55. 10.1016/S0375-9474(02)00751-0 . in2p3-00019874

**HAL Id: in2p3-00019874**

**<https://hal.in2p3.fr/in2p3-00019874>**

Submitted on 29 Oct 2002

**HAL** is a multi-disciplinary open access archive for the deposit and dissemination of scientific research documents, whether they are published or not. The documents may come from teaching and research institutions in France or abroad, or from public or private research centers.

L'archive ouverte pluridisciplinaire **HAL**, est destinée au dépôt et à la diffusion de documents scientifiques de niveau recherche, publiés ou non, émanant des établissements d'enseignement et de recherche français ou étrangers, des laboratoires publics ou privés.

# Quantum propagator approach to heavy-ion fusion

Jing-Dong Bao<sup>1,2</sup> and David Boilley<sup>2</sup>

<sup>1</sup> *Department of Physics, Beijing Normal University, Beijing 100875, China*

<sup>2</sup> *GANIL, BP 55027, 14076 Caen Cedex 05, France*

To appear in Nucl. Phys. A

## Abstract

The real-time path integral propagator approach is used to study the fusion probability of massive nuclei including quantum effect. An analytical expression of the probability to pass over barrier of an inverted harmonic potential is obtained, in which both height and curvature of the barrier are controlled by the neck degree of freedom. The fusion probability of three systems in central collision as a function of the center-of-mass energy are calculated and compared to experimental results. It is shown that the quantum fluctuation enhances the fusion probability at low energies, and the neck fluctuation makes the slope of the fusion probability curve become flatter.

PACS: 25.70.Jj, 05.60.Gg, 03.65.Db

**Keywords:** Fusion probability, massive nuclei, quantum effect, propagator

Dynamics of barrier is of both theoretical and particular interests in many areas of physics, and many works have been done on the subjects of Kramers problem and dissipative tunnelling [1, 2]. Traditional approach to the quantum dissipative decay is the imaginary-time path integral approach within the framework of the system-plus-reservoir model [1-7]. When a particle decays from a metastable state to a true ground state, theory must occur through either a thermally activated barrier crossing or a quantum tunnelling. But, such a theory is not appropriate to solve the inverse problem of the quantum metastable-state decay. Nevertheless, one can introduce exactly the effects of quantum noise on the dynamical system using the real-time influence-functional method [4, 5] in cases where the motion is predominantly deterministic. For sake of simplicity, the model is limited to thermal diffusion over a one-dimensional parabolic potential. Consideration of time-dependent quantum diffusion is still an open question. Results are then applied to the fusion of massive nuclei.

Very recently, Abe et al. [8] obtained an analytical expression for multidimensional fusion probability through solving the Langevin equation, however, realistic numerical calculations were not done and initial distributions of position and momentum of the system were not considered. In the present work, we focus on nearly symmetric reactions, because for these systems, the calculations of the thermal fluctuation model underestimate the fusion probability at low energies [9], and the slope of the fusion probability of the theoretical results as a function of the center-of-mass energy is steeper than that of the experimental data.

The paper is organized as follows: In Sec. 2 we describe the model and derive an expression of the fusion probability with quantum effect in terms of real-time path integral propagator approach, and the neck effect is considered by folding a Gaussian distribution of the neck variable. In Sec. 3 the fusion excitation curves of three typical systems are calculated and compared with experimental data. Finally, the conclusions are summarized

## 2. The model

Since the pioneering work of Feynman-Vernon [3] and Caldeira-Leggett [4, 5], the standard model uses an infinite set of harmonic oscillators for the environment and a bilinear interaction with the system. The Lagrangian of whole system is written as

$$\begin{aligned} L &= L_A + L_B + L_I, \\ L_A &= \frac{p^2}{2M} - V(x), \\ L_B + L_I &= \sum_{i=1}^N \frac{1}{2} \left[ \frac{p_i^2}{m_i} - m_i \omega_i^2 \left( R_i - \frac{c_i}{m_i \omega_i^2} x \right)^2 \right]. \end{aligned} \quad (1)$$

The classical dynamics of the system  $A$  can be described by a generalized Langevin equation from Eq. (1), i.e.,

$$M\ddot{x}(t) + \int_0^t \gamma(t-s)\dot{x}(s)ds + V'(x) = r_1(t), \quad (2)$$

with  $\langle r_1(t) \rangle = 0$  and  $\langle r_1(t)r(s) \rangle = T\gamma(t-s)$ , here  $\gamma(t)$  is the real-time damping kernel function and  $T$  the nuclear temperature.

Our starting point is the real-time path-integral form of the density operator  $\rho(t)$  at any time in the coordinate representation. The reduced density function of the system  $A$  is determined by tracing out all environment coordinates  $\mathbf{R}$  [3-5], i.e.,

$$\begin{aligned} \tilde{\rho}(x, y, t) &= \int d\mathbf{R} \langle x\mathbf{R} | \rho(t) | y\mathbf{R} \rangle = \int dx' dy' d\mathbf{R}' d\mathbf{Q}' d\mathbf{R} \langle x\mathbf{R} | \exp(-iHt/\hbar) | x'\mathbf{R}' \rangle \\ &\quad \cdot \langle y'\mathbf{Q}' | \exp(iHt/\hbar) | y\mathbf{R} \rangle \langle x'\mathbf{R}' | \rho(0) | y'\mathbf{Q}' \rangle. \end{aligned} \quad (3)$$

It is suitable to introduce new variables in order to solve the coupled classical equations of motion for the variables  $x(\tau)$  and  $y(\tau)$ , then we define

$$X(\tau) = x(\tau) + y(\tau), \quad \xi(\tau) = x(\tau) - y(\tau). \quad (4)$$

development of the reduced density of the system through a propagator  $J$  [5], i.e.,

$$\tilde{\rho}(X_f, \xi_f, t) = \int \int dX_i d\xi_i J(X_f, \xi_f, t; X_i, \xi_i, 0) \tilde{\rho}(X_i, \xi_i, 0). \quad (5)$$

We initially have the system in a pure state described by a wave packet centered at the position  $x_0 < 0$  with initial average momentum  $p_0 > 0$ , as well as the fluctuation widths of the position and momentum are  $\lambda$  and  $\mu$ , respectively. The reduced density function is then

$$\tilde{\rho}(X_i, \xi_i, 0) = C_0 \exp\left(\frac{ip_0\xi_i}{\hbar}\right) \exp\left\{-\frac{1}{8\lambda}(X_i - 2x_0)^2 - \frac{\mu}{2\hbar^2}\xi_i^2\right\}, \quad (6)$$

where  $C_0$  is the initial normalization constant.

We assume that the potential is an inverted harmonic potential  $V(x) = \frac{1}{2}M\omega^2x^2$ , which seems reasonable from Fig. 1. Of particular interest, is the expression we obtained for the propagator  $J$  by making  $\xi_f = x_f - y_f = 0$  or  $X_f = 2x_f$ ,

$$J = J_0 \exp\left\{\frac{i}{\hbar}\left[\left(K(t) + \frac{1}{4}M\beta\right)X_i\xi_i - N(t)X_f\xi_i - \frac{1}{\hbar}C(t)\xi_i^2\right]\right\}, \quad (7)$$

where  $J_0$  is an integral constant,  $N$ ,  $K$  and  $C$  are all functions of time and defined by

$$\begin{aligned} N(t) &= \frac{M\beta'}{4\sinh(\frac{1}{2}\beta't)} \exp(\frac{1}{2}\beta't), \\ K(t) &= \frac{1}{4}M\beta' \coth(\frac{1}{2}\beta't), \\ C(t) &= \frac{M\beta}{2\pi} \int_0^\Omega d\nu \nu \coth\left(\frac{\hbar\nu}{2k_B T}\right) \sinh^{-2}(\frac{1}{2}\beta't) \\ &\quad \cdot \int_0^t \int_0^t \sinh[\frac{1}{2}\beta'(t-\tau)] \cos[\nu(\tau-s)] \sinh[\frac{1}{2}\beta'(t-s)] \exp[\frac{\beta}{2}(\tau+s)] d\tau ds. \end{aligned} \quad (8)$$

In Eq. (8),  $\beta' = (\beta^2 + 4\omega^2)^{1/2}$ ,  $\beta$  is the reduced friction coefficient, and  $\Omega$  is a cutoff of high frequency of the Ohmic friction used in this paper.

The reduced density function at any time can be evaluated by substituting Eqs. (6) and (7) into Eq. (5), thus all integrals in Eq. (5) are Gaussian. Here we quote only the final result,

$$\tilde{\rho}(x_f, 0, t) = C_f \exp\left[-\frac{(x_f - \langle x_f(t) \rangle)^2}{2\sigma_{x_f}^2(t)}\right], \quad (9)$$

$$\begin{aligned}\langle x_f(t) \rangle &= \frac{[\frac{1}{4}M\beta + K(t)]x_0 + \frac{1}{2}p_0}{N(t)}, \\ \sigma_{x_f}^2(t) &= \frac{2C(t)\hbar + \mu + 4\lambda[\frac{1}{4}M\beta + K(t)]^2}{N(t)^2}.\end{aligned}\quad (10)$$

Namely,

$$\begin{aligned}\langle x_f(t) \rangle &= \exp(-\frac{\beta}{2}t) \left\{ x_0 \left[ \frac{\beta}{\beta'} \sinh(\frac{1}{2}\beta't) + \cosh(\frac{1}{2}\beta't) \right] \right. \\ &\quad \left. + \frac{2p_0}{M\beta'} \sinh(\frac{1}{2}\beta't) \right\},\end{aligned}\quad (11)$$

and for the variation of the position, the only surviving terms proportional to  $\exp[(\beta' - \beta)t]$  are kept,

$$\begin{aligned}\sigma_{x_f}^2(t) &= \left[ \frac{M\beta'}{4 \sinh(\frac{1}{2}\beta't)} \right]^{-2} \exp(-\beta t) \left\{ \frac{\hbar M\beta}{\pi} \int_0^\Omega \frac{\nu d\nu \coth(\frac{\hbar\nu}{2k_B T})}{a^2 + \nu^2} \right. \\ &\quad \left. + \mu + \lambda M \left[ \beta + \beta' \coth(\frac{1}{2}\beta't) \right]^2 \right\},\end{aligned}\quad (12)$$

where  $a = (\beta' - \beta)/2 > 0$ . The center of the peaked  $\tilde{\rho}(x_f, 0, t)$  follows the motion of a classical Brownian particle and its width is enlarged by the quantum fluctuation.

In this model the probability at a given time that the particle has passed over the barrier is determined by

$$P(x_0, p_0, t) = \frac{\int_0^\infty \tilde{\rho}(x_f, 0, t) dx_f}{\int_{-\infty}^\infty \tilde{\rho}(x_f, 0, t) dx_f} = \frac{1}{2} \operatorname{erfc} \left( -\frac{\langle x_f(t) \rangle}{\sqrt{2}\sigma_{x_f}(t)} \right). \quad (13)$$

For long times, the value of  $\langle x_f(t) \rangle / \sigma_{x_f}(t)$  is finite, we have

$$\lim_{t \rightarrow \infty} \frac{\langle x_f(t) \rangle}{\sqrt{2}\sigma_{x_f}(t)} = \frac{\frac{1}{2}(\beta + \beta')x_0 + p_0/M}{\left\{ \frac{2\hbar\beta}{M\pi} \int_0^\Omega \frac{\nu d\nu}{a^2 + \nu^2} \coth(\frac{\hbar\nu}{2k_B T}) + \frac{2\mu}{M^2} + \frac{1}{2}\lambda(\beta + \beta')^2 \right\}^{1/2}}. \quad (14)$$

Eq. (13) with (12) is the main result of this paper. Let us analyze the behavior of Eq. (14). When  $2k_B T > \hbar\Omega \gg \hbar a$ , we write an approximation to the quantum term in Eq. (14),

$$\begin{aligned}\frac{2\hbar\beta}{M\pi} \int_0^\Omega \frac{\nu d\nu}{a^2 + \nu^2} \coth \left( \frac{\hbar\nu}{2k_B T} \right) &\approx \frac{2\beta k_B T}{Ma} \left[ 1 + \frac{1}{\sqrt{6}} \frac{\hbar a}{k_B T} \right. \\ &\quad \left. - \frac{1}{12} \left( \frac{\hbar a}{k_B T} \right)^2 + \frac{1}{48\sqrt{6}} \left( \frac{\hbar a}{k_B T} \right)^3 + \dots \right],\end{aligned}\quad (15)$$

becomes  $\hbar\beta(M\pi)^{-1}\ln(1+\Omega^2/a^2)$  and is finite [10].

### 3. Results and discussion

Now we apply the quantum diffusion formula [Eqs. (13) and (14)] to massive heavy-ion fusion. Here, the shape of nucleus is described by the two-center parameterization with two collective variables  $\{x, \epsilon\}$ , in which  $x$  is the distance between the two colliding nuclei and  $\epsilon$  ( $0 \leq \epsilon \leq 1$ ) the neck parameter. The inertia is adopted with the Werner-Wheeler approximation, the wall-and-window one-body dissipation is used for the friction, as well as the potential energy is calculated by the liquid-drop model.

In order to determine the nuclear temperature, we will assume that all the remaining energy is totally dissipated around the fusion saddle points [8]. Therefore, with a level density  $a_{lev}$ , we have  $a_{lev}T^2 = E_{cm} + Q - V_b$ , neglecting the collective kinetic energy. Here  $V_b$  is the energy difference of the fusion saddle point and the ground state. The initial kinetic energy of the system when the two nuclei being in the contact shape is given by

$$K = \frac{1}{2m}p_0^2 = E_{cm} + Q - V_c - a_{lev}T_0^2. \quad (16)$$

Here  $E_{cm}$  is the center-of-mass energy,  $Q$  denotes the  $Q$ -value of the reaction,  $V_c$  is the energy difference between the contact shape and the ground state of the compound nucleus, and  $T_0$  is the initial excitation temperature determined from the nuclear surface friction model.

In the approaching phase of the heavy-ion fusion, the neck length of two colliding nuclei is expected to grow and fluctuate as time goes, thus the height, location and curvature of the fusion saddle also change, as shown on Fig. 1. Since  $x$  and  $\epsilon$  degrees of freedom are to be simultaneously taken into consideration when calculating the quantum diffusion, an effective diffusion over a 1-D barrier is considered. Thus the fusion probability is calculated

$$P_{fus}(E_{cm}) = \int_0^1 P(x_0, p_0, t \rightarrow \infty) w(\epsilon) \delta(a\epsilon + bx_0 + c) d\epsilon, \quad (17)$$

where the distribution of the neck variable  $\epsilon$  is assumed to be a Gaussian function,

$$w(\epsilon) = (2\pi\sigma_\epsilon^2)^{-1/2} \exp[-(\epsilon - \bar{\epsilon})^2/(2\sigma_\epsilon^2)]. \quad (18)$$

Here  $\bar{\epsilon}$  and  $\sigma_\epsilon^2$  are determined by the solution of the neck evolution equation [10],

$$\ddot{\epsilon}(t) + \gamma_\epsilon \dot{\epsilon}(t) - \frac{1}{m_\epsilon} f_\epsilon = \sqrt{2\gamma_\epsilon T/m_\epsilon} r_2(t), \quad (19)$$

where  $m_\epsilon$  and  $\gamma_\epsilon$  are the mass and reduced friction of the fusion system along the neck degree of freedom at the barrier, as well as  $\langle r_2(t) \rangle = 0$  and  $\langle r_2(t)r_2(t') \rangle = \delta(t - t')$ . Eq. (17) means that the fusion starts from the various configurations of the reacting nuclei which is described by the distribution  $\omega(\epsilon)$  of the neck variable.

In Fig. 1, we plot the deformation potential energy for the reaction  $^{100}\text{Mo} + ^{100}\text{Mo}$  as a function of the elongation coordinate  $x$  for different neck parameters  $\varepsilon$ . The black points correspond to the cases of zero-radius neck, namely, the contact shapes. It shows clearly that the behavior of the barrier depends on the neck degree of freedom. In the shape model of the two-center parameterization, the distance of mass center of two fusing nuclei increases and then the Coulomb repulsion energy decreases when the value of  $\epsilon$  decreases at the contact points, thus the deformation energy of the system decreases. From this figure, we observe that the contact point is close to the fusion saddle for the symmetrical systems near  $A = 200$ , so that the values of mass and friction can be chosen at the fusion saddle, as well as the curvature of the barrier is also treated reasonably to be a constant, though it is a function of the neck variable. Within the two-dimensional space of  $x$  and  $\epsilon$ , the averaging path of the particle shall drift off the highest potential energy barrier, namely, diffusion over the fusion saddle and simultaneously falling along the  $\epsilon$ -direction.



reaction systems:  $^{100}\text{Mo}+^{100}\text{Mo}$ ,  $^{86}\text{Kr}+^{123}\text{Sb}$ , and  $^{96}\text{Zr}+^{124}\text{Sn}$  for which the phenomenon of the fusion hindrance appears. Experimental data are taken from Refs. [12-15] and for the present calculations with quantum effects,  $\Omega = 100a$ . The fusion hindrance is defined by the difference between the energy corresponding to  $P_{fus} = 0.5$  and the Bass barrier. Theoretically,  $P_{fus} = 0.5$  when  $\lim_{t \rightarrow 0} \langle x_f(t) \rangle = 0$ , see eq. (13). Then, at this point, the quantum fusion probability is the same as the classical one and the hindrance calculated by the quantum diffusion equals to the classical one. Because the quantum width is larger than the classical one, fusion probability is enhanced by the quantum noise at low energies. The lower the energy is, the larger the effect is, naturally. At high energies, the quantum fusion probability is lower than the classical one, but the difference is very small, as expected. The effects of neck folding are discussed in Ref. [11].

#### 4. Summary

In this paper, we have studied the diffusion over a 1-D parabolic barrier, including quantum noise and derived an exact over-passing probability formula that is applied to the study of the fusion of massive nuclei. The results shows that the quantum fluctuations enhance the fusion probability at low energies. For comparison with experimental data, neck degree of freedom is included by folding the initial distribution. Local harmonic approximation for the propagator consisting of the coordinate-dependent mass and friction as well as a realistic potential should be considered further.

#### ACKNOWLEDGMENTS

We would like to thank Y. Abe for providing helpful suggestions and J.D.B thanks the GANIL for its warm hospitality, during visit where part of this work was done. This work

## References

- [1] P. Hänggi, P. Talkner, M. Borkover, Rev. Mod. Phys. 62 (1990) 251.
- [2] U. Weiss, *Quantum Dissipative Systems* (World Scientific, Singapore, 1993).
- [3] R.P. Feynman, F.L. Vernon, Ann. Phys. (N.Y.) 24 (1963) 118; R.P. Feynman and A.R. Hibbs, *Quantum Mechanics and Path Integrals* (McGraw-Hill Book Company, New York, 1965).
- [4] A.O. Caldeira and A.J. Leggett, Phys. Rev. Lett. 46 (1981) 211.
- [5] A.O. Caldeira and A.J. Leggett, Physica A 121 (1983) 587; Ann. Phys. (N.Y.) 149 (1983) 374.
- [6] H. Grabert, P. Olschowski, U. Weiss, Phys. Rev. B 36 (1987) 1931.
- [7] J. Ankerhold, H. Grabert, G.-L. Ingold, Phys. Rev. E 51 (1995) 4267.
- [8] Y. Abe, D. Boilley, B.G. Giraud, T. Wada, Phys. Rev. E 61 (2000) 1125.
- [9] C.E. Aguiar, V.C. Barbosa, R. Donangelo, Nucl. Phys. A 517 (1990) 205.
- [10] H. Hofmann, Phys. Rep. 284 (1997) 137.
- [11] J.D. Bao, Y. Abe, D. Boilley, “Neck folding model of fusion of massive nuclei”, to be published.
- [12] K.H. Schmidt and W. Morawek, Rep. Prog. Phys. 54 (1991) 949.
- [13] W. Reisdorf, J. Phys. G 20 (1994) 1297.

- and C.-C. Sahm, Nucl. Phys. A 452 (1986) 173.
- [15] A.B. Quint, W. Reisdorf, K.-H. Schmidt, P. Armbruster, F.P. Heßberger, S. Hofmann, J. Keller, G. Münzenberg, H.-G. Clerc, W. Morawek, C.-C. Sahm, Z. Phys. A 346 (1993) 119.

**FIG. 1.** The deformation potential energy as a function of the elongation coordinate for different neck parameters  $\epsilon = 1.0, 0.8, 0.6, 0.4$ , and  $0.2$  from top to bottom. Here the black points correspond to the contact shapes of two fusing nuclei,  $R_0$  is the radius of the compound nucleus.

**FIG. 2.** Calculated fusion probability of  $^{100}\text{Mo} + ^{100}\text{Mo}$  as a function of the center-of-mass energy. The solid line is the present quantum diffusion result, the dotted line is the classical diffusion result, and the dashed line is the 1-D classical diffusion result of Ref. [8] without neck folding. The points are the experimental data.

**FIG. 3.** Calculated fusion probability of  $^{86}\text{Kr} + ^{123}\text{Sb}$  as a function of the center-of-mass energy. The symbols are the same as Fig. 2.

**FIG. 4.** Calculated fusion probability of  $^{96}\text{Zr} + ^{124}\text{Sn}$  as a function of the center-of-mass energy. The symbols are the same as Fig. 2.

FIG.1

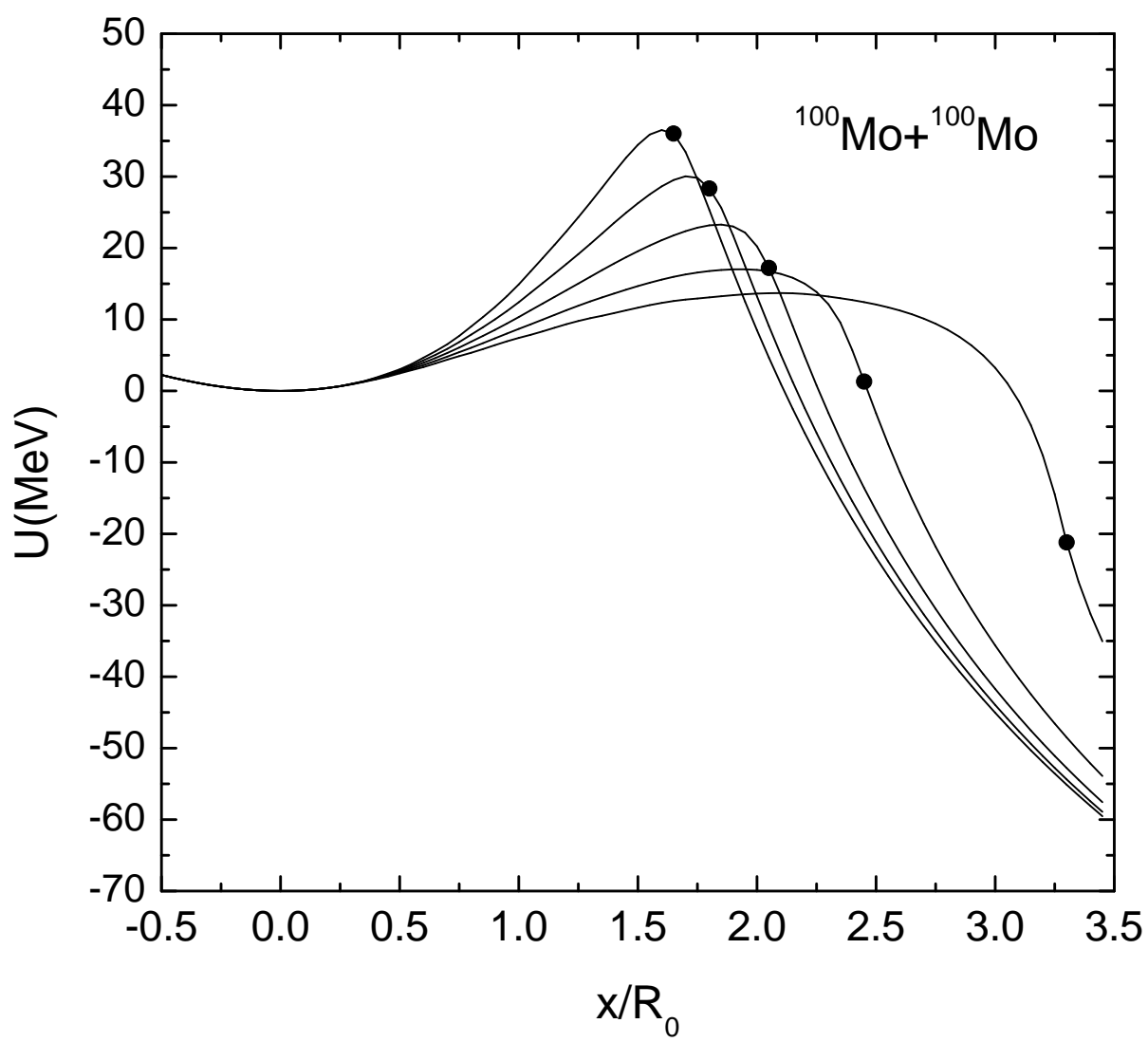


FIG.2

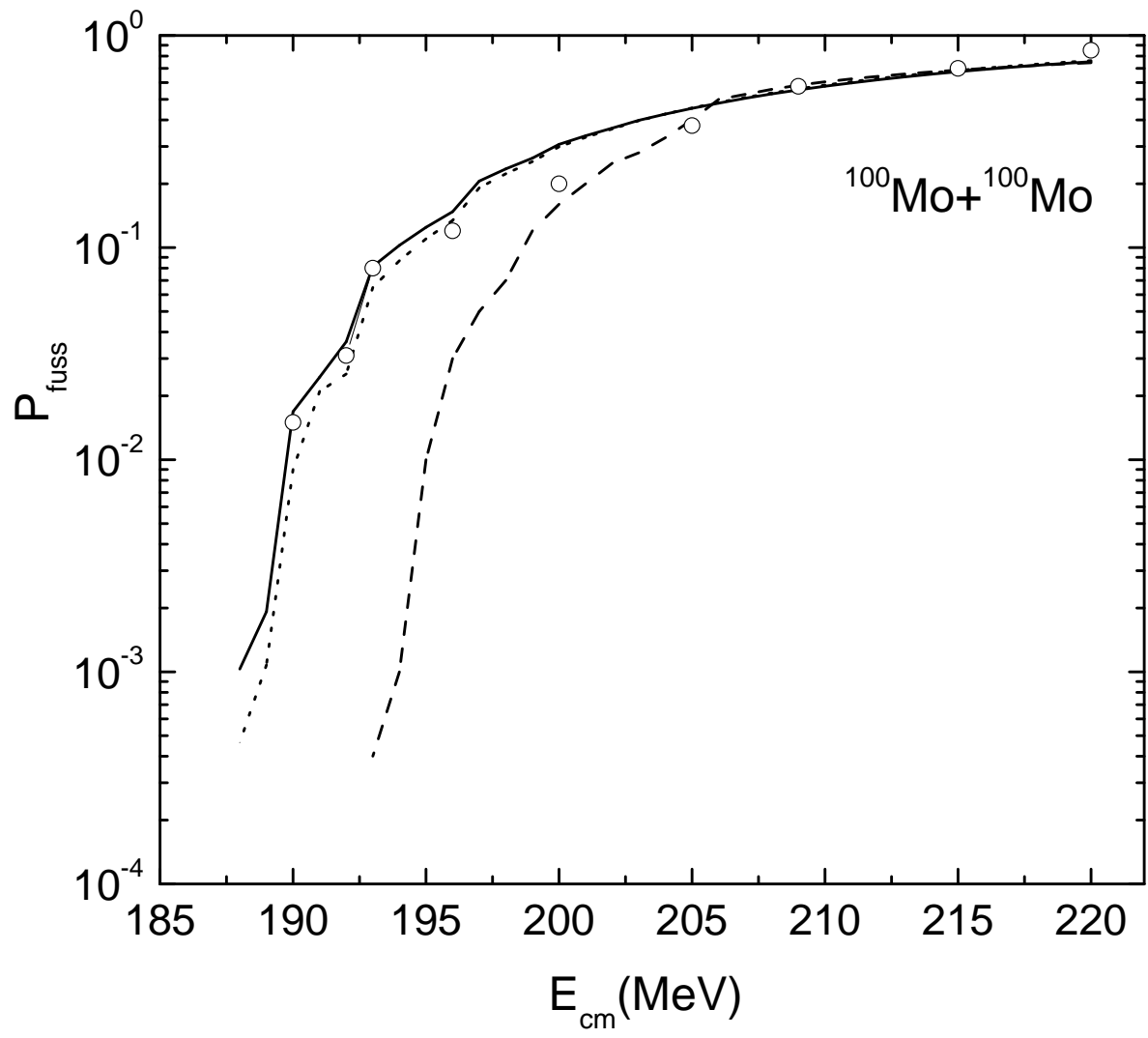


FIG.3

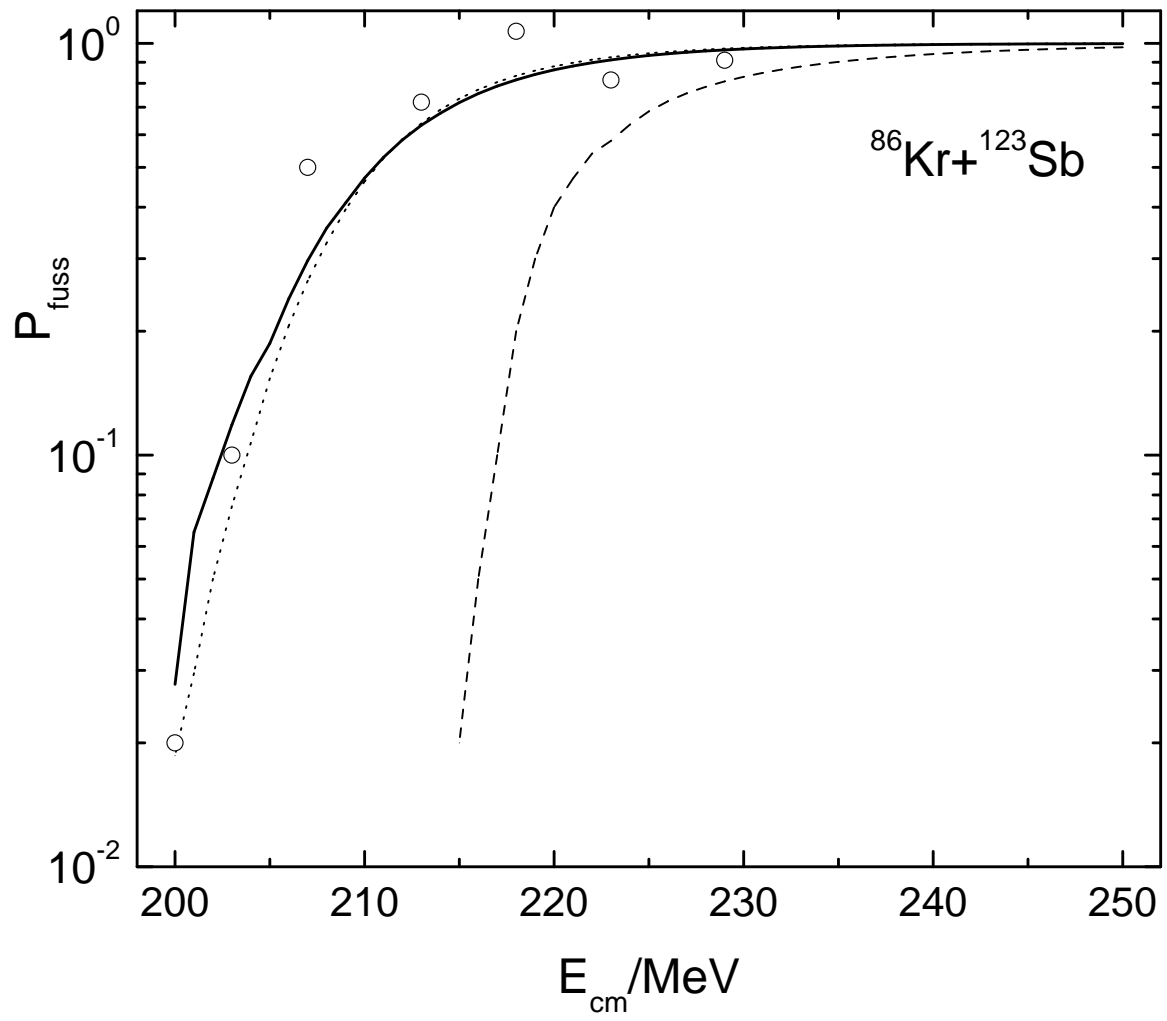


FIG.4

